National Institute of Standards & Technology

Report of Investigation

Reference Material 8671

NISTmAb, Humanized IgG1κ Monoclonal Antibody

Lot No. 14HB-D-002

The NIST Monoclonal Antibody (NISTmAb) Reference Material (RM) is a recombinant humanized IgG1κ expressed in murine suspension culture and has undergone biopharmaceutical industry standard upstream and downstream purification to remove process related impurities. It is an ≈150 kDa homodimer of two light chain and two heavy chain subunits linked through both inter- and intra-chain disulfide bonds. The molecule has a high abundance of N-terminal pyroglutamination, C-terminal lysine clipping, and glycosylation of the heavy chains. The protein also has low abundance post-translational modifications including methionine oxidation, deamidation, and glycation. These and other product quality attributes were extensively characterized in the ACS Symposium Series for the initial batch of interim material, used as the primary standard (PS) herein [1-3]. A thorough expansion on the specific protocols and results briefly described in this Report of Investigation can be found in references [4-8].

This RM is intended primarily for use in evaluating the performance of methods for determining physicochemical and biophysical attributes of monoclonal antibodies. It also provides a representative test molecule for development of novel technology for therapeutic protein characterization. This RM can be used for a variety of purposes that may include system suitability tests, establishing method or instrument performance and variability, comparing changing analytical test methods, and assisting in method qualification. A unit of RM 8671 consists of one cryovial containing 800 µL of 10 mg/mL IgG1κ monoclonal antibody in 12.5 mmol/L L-histidine, 12.5 mmol/L L-histidine HCl (pH 6.0).

Reference Mass Concentration Value: A NIST reference value is a non-certified value that is the best estimate of the true value based on available data; however, the value does not meet the NIST criteria for certification and is provided with associated uncertainty that may reflect only measurement precision, may not include all sources of uncertainty, or may reflect a lack of sufficient statistical agreement among multiple analytical methods [9]. The mass concentration value listed in Table 3 is based on measured decadic attenuance, *D*, at 280 nm. The decadic attenuance, *D*, is computed as the negative logarithm (base 10) of the transmittance, and is analogous to absorbance except for the inclusion of scattering and luminescence effects upon the radiant power exiting the sample [10]. Concentration of the NISTmAb was determined by using a theoretical extinction coefficient (ε) of 1.42 mL · mg^{-1} · cm^{-1} [11-12] and a glycan mass fraction correction factor of 0.977 [11]. The contributions to the uncertainty associated with this mass concentration measurement can be found in Table 4.

Physicochemical Reference Values: Physicochemical attributes of RM 8671 were evaluated using qualified size exclusion chromatography (SEC), capillary sodium dodecyl sulfate electrophoresis (CE-SDS), and capillary zone electrophoresis methods (CZE). These analytical assays were qualified using the primary standard (PS) in order to establish method performance criteria. Qualification exercises were modeled after the ICH Q2(R1) guidelines for method validation and included assessment of linearity, limit of detection (LOD)/limit of quantification (LOQ), range, and precision (repeatability and some intermediate precision). Physicochemical reference values provided in Tables 5, 6, and 7 were assigned by analyzing Lot 14HB-D-002 with each qualified method (SEC, CE-SDS, and CZE) while bracketing analysis with an instrument qualification (IQ) standard and the PS to ensure system suitability. Both the IQ standard and PS were required to pass pre-defined method performance criteria from method qualification.

Overall direction and coordination of technical measurements were performed by K. Yandrofski and J.E. Schiel of the NIST Biomolecular Measurement Division.

Michael J. Tarlov, Chief
Biomolecular Measurement Division

Gaithersburg, MD 20899
Steven J. Choquette, Director
Office of Reference Materials

Report Issue Date: 18 December 2020
Report Revision History on Last Page

Information Values: Additional physicochemical characterization methods including dynamic light scattering (DLS) and flow imaging analysis were also applied to RM 8671 and directly compared to data collected for the PS. Informational values are considered to be of interest and use to the RM user, but insufficient information is available to adequately assess the uncertainty associated with the value or only a limited number of analyses were performed. Information values cannot be used to establish metrological traceability.

Identity: Ultrahigh-performance liquid chromatography coupled with online ultraviolet (UV) and tandem mass spectrometry detection (UHPLC-UV-MS/MS) was also applied to this RM. Parallel sample preparations of PS were directly compared with respect to visual appearance and peak retention times of the total ion chromatogram (TIC) and the UV peptide map at 214 nm. Collision induced dissociation MS/MS peak identifications corresponding to peptides derived from the putative NISTmAb sequence were used to confirm identity and assure comparability with the PS.

Expiration of Value Assignment: **RM 8671 Lot 14HB-D-002** is valid, within the measurement uncertainty specified, until **29 April 2022**, provided the RM is handled and stored in accordance with instructions given in this report (see "Instructions for Storage and Use"). The value assignment is nullified if the RM is damaged, contaminated, or otherwise modified. NIST does not endorse or warrant the homogeneity, stability, purity, or reported values for materials or derivatives thereof that are not branded with an official NIST label.

Maintenance of RM: NIST will monitor this RM over the period of its validity. If substantive technical changes occur that affect the value assignment before the expiration of this report, NIST will notify the purchaser. Registration (see attached sheet or register online) will facilitate notification.

Value assignment measurements were performed by J.E. Schiel, K. Yandrofski, S. Telikepalli, and J. King of the NIST Biomolecular Measurement Division, and P. DeRose of the NIST Biosystems and Biomaterials Division; and A.H. Turner, T. Formolo, formerly of NIST, and were performed at NIST (Gaithersburg, MD) or the Institute of Bioscience and Biotechnology Research (Rockville, MD).

Acquisition of the material was performed by J.E. Schiel and M. Tarlov of the NIST Biomolecular Measurement Division and H. Zube of the NIST Technology Partnerships Office.

Additional technical guidance was provided by B. Lang, J. Travis, and A. Urbas of the NIST Biosystems and Biomaterials Division and management support was provided by M. Tarlov, K. Phinney, J. Marino, and D. Ripple of the NIST Biomolecular Measurement Division, and K. Cole of the NIST Biosystems and Biomaterials Division.

Statistical analysis was provided by A. Heckert of the NIST Statistical Engineering Division.

Support aspects involved with the issuance of this RM were coordinated through the NIST Office of Reference Materials.

NOTICE AND WARNINGS TO USERS

RM 8671 IS INTENDED FOR RESEARCH USE. NOT INTENDED FOR ANIMAL OR HUMAN CONSUMPTION, CLINICAL TESTING, OR THERAPEUTIC USE. As a general rule, personal protective equipment should always be worn during any laboratory procedure. This includes, but is not limited to safety goggles, gloves, and a laboratory jacket.

INSTRUCTIONS FOR STORAGE AND USE

Storage: This RM is packaged and supplied to the user in internal threaded polypropylene cryovials. Each vial contains 800 µL of 10 mg/mL IgG1κ monoclonal antibody in 12.5 mmol/L L-histidine, 12.5 mmol/L L-histidine HCl (pH 6.0). The RM is shipped on dry ice and should remain frozen during shipment. The material should be stored in a frozen state at −80 °C immediately upon receipt. A series of stability samples were evaluated to determine the optimum and most extreme storage conditions under which the sample will likely retain its physicochemical performance for a given method. In all cases, storage of the material at −80 °C is preferred. However, if aliquot preparation and/or storage at other than recommended conditions are necessary, the maximum storage time recommended under given conditions and for certain intended uses is listed in Table 1 for reference values and Table 2 for informational values and peptide mapping.

Table 1. Method-Based Alternate Storage Conditions for RM 8671 Reference Value Determinations[a]

Method	Attribute	Recommended Storage	Max F/T[b] (cycles) −80 °C	−20 °C	Max Storage 4 °C (days)	Control Range
UV[c]	Concentration	−80 °C	5	5	28	± 2u_c
SEC[d]	Monomeric Purity	−80 °C	5	5	7	± 3u_c
nrCE-SDS[e]	Monomeric Purity	−80 °C	5	5	28	± 3u_c
rCE-SDS[f]	Glycan Occupancy, Thioether Content	−80 °C	5	5	28	± 3u_c
CZE[g]	Charge Purity	−80 °C	5	5	28	± 3u_c

[a] Measured values are expected to be within the indicated control range, where u_c is the combined standard uncertainty, based on the alternate storage conditions listed for each individual method.
[b] Freeze/Thaw cycles (F/T)
[c] Ultraviolet visible spectrophotometry (UV)
[d] Size exclusion chromatography (SEC)
[e] Non-reduced capillary sodium dodecyl sulfate electrophoresis (nrCE-SDS)
[f] Reduced capillary sodium dodecyl sulfate electrophoresis (rCE-SDS)
[g] Capillary zone electrophoresis (CZE)

Table 2. Method-Based Alternate Storage Conditions for RM 8671 Information Value Determinations and Peptide Mapping

Method	Attribute	Recommended Storage	Max F/T[a] (cycles) −80 °C	−20 °C	Max Storage 4 °C (days)
FI[b]	Subvisible Particle Content	−80 °C	0	0	28
DLS[c]	Hydrodynamic Diameter	−80 °C	5	5	28
Peptide Map	Identity	−80 °C	ND[d]	ND	ND

[a] Freeze/Thaw cycles (F/T)
[b] Flow imaging analysis (FI)
[c] Dynamic light scattering (DLS)
[d] Not determined

Storage Stability Evaluation: Storage stability evaluation was performed on RM 8671 Lot 14HB-D-001 and extrapolated here to Lot 14HB-D-002. Vials reserved for Freeze/Thaw (F/T) cycle studies were thawed at room temperature, gently inverted five times, and spun briefly in a mini-centrifuge. The initial thaw of the material was considered as thaw zero. Samples were then subjected to an additional one to five F/T cycles with freeze temperature set at −80 °C for one sample set and −20 °C for a second sample set.

Vials reserved for accelerated stability were thawed at room temperature (at the appropriate time point), gently inverted five times, and spun briefly in a mini-centrifuge. Samples were then placed at 4 °C in the dark, room temperature (22 °C) in the light, and 40 °C in the dark to produce samples subjected to total incubation times of 1, 4, 7, 14, and 28 days. Vials were then frozen at −80 °C until analysis.

F/T samples were tested (at a minimum) after undergoing an additional one to five F/T cycles with freeze temperature at −80 °C or −20 °C. Accelerated stability samples were initially tested using each method described above at the 0, 1, 7, and 28 day time points. Additional time points were analyzed in some cases where deemed necessary.

For Table 1, control charts for alternative storage stability evaluations were prepared for the methods described. Each method control chart utilized uncertainty parameters that were centered on the mean value determined. Maximum storage F/T cycles and maximum storage time at a given temperature were set (for each method individually) as the most extreme data point that remained within the control range.

Instructions for Use: The vial should be removed from the −80 °C freezer and thawed at room temperature for approximately 30 minutes or until no residual ice crystals remain. Once thawed, the vial should be gently inverted five times to alleviate any concentration gradients that may have formed during the freezing process. The vial should then be quickly spun in a mini-centrifuge to settle any solution that may otherwise remain adhered to the lid or internal threads of the vial. Once opened, the vial contents should be used immediately and/or stored at the pre-defined conditions listed in Table 1 according to the intended use of the material.

Preparation of Dilutions: Protein solutions of lower concentration may be prepared by transferring an aliquot and diluting to the appropriate volume. Diluents are not furnished with the RM; however, aqueous diluents such as the formulation buffer (12.5 mmol/L L-histidine, 12.5 mmol/L L-histidine HCl, pH 6.0) may be used. Solubility and stability of the material have not been fully tested by NIST under dilute or concentrated conditions and therefore may not conform to expectation in the analytical assays described herein.

SOURCE, PREPARATION, AND ANALYSIS[1]

Source and Preparation: This RM was received as a bulk substance prepared using mammalian cell culture and downstream processing representative of industry state-of-the-art. Multiple bulk substance containers were first homogenized to form the 14HB batch. Aliquots of 1 L each were made from the homogenized bulk and designated as individual lots. A single lot (14HB-002) was then diluted 10 fold in USP grade formulation buffer (12.5 mmol/L L-histidine, 12.5 mmol/L L-histidine HCl, pH 6.0) and 800 µL aliquots placed into internally threaded screw top. Vials were placed in racks of 96 units each for storage at –80 °C. Sample processing was completed in a sterile environment using pre-sterilized single-use equipment and/or in a class 100 000 cleanroom environment.

Homogeneity Analysis: The homogeneity assessment was made at the time value assignment analyses were performed. A stratified sampling plan was devised to test for homogeneity across the lot of vials. There was no apparent trend in the data when plotted against the sequence in which the samples were prepared.

REFERENCE MASS CONCENTRATION VALUE ASSIGNMENT BY UV-VISIBLE SPECTROPHOTOMETRY FOR PROTEIN CONCENTRATION

Sample Handling Prior to Analysis: Each vial was thawed at room temperature, gently inverted five times, and spun briefly in a mini-centrifuge.

Measurement of NISTmAb Concentration by UV-Visible Spectrophotometry at 280 nm: Concentration of protein material is often performed using UV-Visible spectrophotometry wherein the measured absorbance is assumed to be equivalent to the decadic attenuance. The decadic attenuance, D, is computed as the negative logarithm (base 10) of the transmittance, and is analogous to absorbance except for the inclusion of scattering and luminescence effects upon the radiant power exiting the sample [9]. Concentrations reported are based on decadic attenuance at 280 nm (D280).

Reference value assignment was performed using a 0.5 mm path length quartz cuvette. The path length b was measured by the NIST Dimensional Metrology Group using a coordinate measuring machine with a fiber probe having a tip with an ellipsoidal geometry. Primary decadic attenuance measurements of the NISTmAb were measured using the MML Transfer Spectrophotometer, which is traceable to the national reference instrument for absorbance (HAS II). Traceability is achieved using transfer standards SRMs 2034 *Holmium Oxide Solution Wavelength Standard (240 nm to 650 nm)*; *Glass Filters for Spectrophotometry*: 930, 1930, 2930; and 2031 *Metal-on-Fused-Silica Neutral Density Filters (250 nm to 635 nm)*. Calibration of the wavelength scale was done using SRM 2034. Control charts for photometric accuracy use SRMs 930 (visible), 1930 (visible) and 2031 (UV and visible).

[1] Certain commercial equipment, instruments, or materials are identified in this certificate to adequately specify the experimental procedure. Such identification does not imply recommendation or endorsement by the National Institute of Standards and Technology, nor does it imply that the materials or equipment identified are necessarily the best available for the purpose.

Metrological traceability is to the decadic logarithm of the derived SI unit of regular spectral transmittance through the NIST Transfer Spectrophotometer, which is qualified against the HAS II National Spectrophotometer via control standard SRM 2031 at 280 nm. The concentration was determined for each of ten vials (retrieved from separate racks based on a stratified sampling plan) from Lot 14HB-D-002 based on Equation 1.

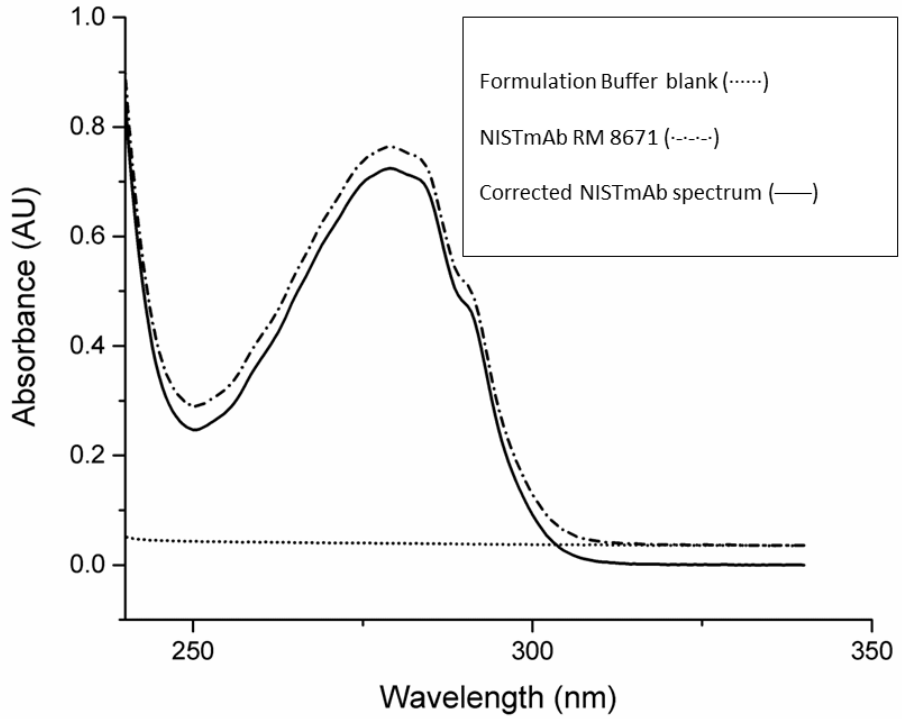

Figure 1. This is a representative spectrum obtained from a vial retrieved from Rack 1 of Lot 14HB-D-002. The decadic attenuance spectra were measured from 240 nm to 340 nm, at a scan rate of 20 nm/min and wavelength interval of 0.5 nm.

NISTmAb samples were measured directly without further dilution or other preparation steps and formulation buffer was used as the blank. Decadic attenuance measurement of the samples was made using the same cuvette as the blank. This blank absorbance reading at 280 nm was subtracted from each RM sample decadic attenuance reading at 280 nm to provide a corrected D280 (D_{corr}). Concentration of the NISTmAb was determined utilizing a theoretical extinction coefficient (ε) of 1.42 mL · mg^{-1} · cm^{-1} [11]. The equation used for calculation of the concentration (C) is displayed in Equation 1.

$$C = \frac{D_{\mathrm{corr}}}{\varepsilon \cdot b} \tag{1}$$

Reference Mass Concentration Value: The reference value listed in Table 3 is based specifically on measured decadic attenuance at 280 nm assuming a theoretical extinction coefficient (ε) of 1.42 mL · mg^{-1} · cm^{-1} [11]. This value was calculated according to the method reported by Pace et al. [*12*], and further corrected for glycan mass fraction via a correction factor of 0.977 [11]. Uncertainty associated with the theoretical extinction coefficient has not been fully evaluated and is not included in the uncertainty evaluation; therefore, the reported value is not traceable to the SI unit of mass. Metrological traceability is to the decadic logarithm of the derived SI unit of regular spectral transmittance through the NIST Transfer Spectrophotometer, which is qualified against the HAS II National Spectrophotometer via control standard SRM 2031 at 280 nm. The concentration was determined for each of 10 vials (retrieved from separate racks based on a stratified sampling plan) from Lot 14HB-D-002 based on Equation 1.

The combined standard uncertainty and expanded uncertainty provided in Table 3 express both the within-method uncertainty and Type B components related to the analysis (described in the following section), consistent with the ISO/JCGM Guide [13]. The expanded uncertainty is calculated as $U = ku_c$, where u_c is intended to represent, at the level of one standard deviation, the effects of the combined components of uncertainty, and $k = 2$ was used as the coverage factor.

Table 3. Reference Mass Concentration Value for RM 8671 Lot 14HB-D-002 by UV-Vis spectrophotometry (n = 10 vials).

Average Concentration (mg/mL)	Standard Type A Uncertainty, u_A (mg/mL)	Combined Standard Uncertainty, u_c (mg/mL)	Expanded Uncertainty, U (%)	Coverage Factor, k
10.003	0.0176	0.0441	0.0882	2

Evaluation of Uncertainty for UV-Visible Spectrophotometry Measurements: The concentration was determined for each of 10 vials (retrieved from separate racks based on a stratified sampling plan) based on Equation 1. Standard Type A uncertainty is reported as the measured standard deviation (u_A) of the resulting concentration (as calculated based on Equation 1 with no propagation of error). Uncertainty associated with the theoretical extinction coefficient has not been fully evaluated and is not included in the uncertainty evaluation; therefore, the reported value is not traceable to the SI unit for mass. However, there are a number of additional factors that contribute to the combined standard uncertainty in measured decadic attenuance. The Transfer Spectrophotometer (TS) is qualified against the NIST High Accuracy Spectrophotometer (HAS II) on a quarterly basis. Qualification of the TS at 280 nm is made through measurements on SRM 2031 absorbance filter on the TS, an SRM which was originally certified on the HAS II. Determination of the expanded uncertainty for a TS measurement of SRM 2031 is described in reference [14]. Contributions to the combined standard uncertainty based on this transfer control measurement include the standard uncertainty of a single TS measurement of the SRM 2031 filter determined by simple replication (u_x), the combined standard uncertainty for the SRM 2031 reference standard as measured on the HAS II (u_{ref}), and the bias of the transfer instrument (vs. HAS II) and uncertainty associated with the bias determination (δ and u_δ, respectively).

Multiple uncertainty contributions to the combined standard uncertainty in D_{corr} were utilized in the combined standard uncertainty calculation, including: (1) the measured standard deviation of the decadic attenuance measurements (u_{Dm}), contributions to uncertainty in photometric accuracy (u_x, u_{ref}, u_δ and δ), and the additional uncertainty to photometric accuracy as a result of the wavelength uncertainty (u_w). Traceability is ensured by including uncorrected bias in the measurement uncertainty rather than by bias correction [15-16]. The bias itself must therefore be added to the expanded uncertainty in the decadic attenuance [15-16]. SRM 2031 utilized a coverage factor of 2; therefore, the combined standard uncertainty associated with the decadic attenuance is given by Equation 2.

$$u_D = \frac{|\delta| + 2\sqrt{u_{Dm}^2 + u_w^2 + u_x^2 + u_\delta^2 + u_{ref}^2}}{2} \tag{2}$$

The path length for the BL05A cuvette was measured previously by the NIST Dimensional Metrology Group using a Coordinate Measuring Machine fitted with a fiber probe as well as using interference fringes in the near-infrared, resulting in an additional B-type contribution to the error (u_b). The uncertainty contribution associated with the theoretical extinction coefficient has not been fully evaluated. Instead the extinction coefficient has been utilized here as a constant, accepted industry norm value. Hence, the mass concentration is reported herein as a reference value. The values utilized for the combined standard uncertainty budget are included in Table 4. Propagation of the combined A- and B-type uncertainties through Equation 1 results in the combined standard uncertainty associated with the concentration measurement as given in Table 3.

Table 4. Uncertainty Components for Reference Mass Concentration Value Assignment for RM 8671 Lot 14HB-D-002

Uncertainty Components	Symbol	Value[(a)]	Uncertainty (Type)
Standard uncertainty of the measured decadic attenuance (Lot 14HB-D-002)	u_{Dm}	0.001273805[(b)]	Type A
Standard uncertainty associated with wavelength accuracy	u_w	0.001	Type B
Standard uncertainty of a single TS measurement on SRM 2031	u_x	0.000049	Type B
Combined standard uncertainty of SRM 2031	u_{ref}	0.0021	Type B
Standard uncertainty of the bias versus HAS II	u_δ	0.000261	Type B
Bias in transmittance density versus the HAS II	δ	0.00104	Type B
Combined standard uncertainty of the path length	u_b	0.000015[(c)]	Type B

[(a)] Unless otherwise noted, value is reported as arbitrary units (AU).
[(b)] Value is unitless.
[(c)] Value is reported in centimeters.

PHYSICOCHEMICAL REFERENCE VALUES

Sample Handling Prior to Analysis: Each vial was thawed at room temperature, gently inverted five times, and spun briefly in a mini-centrifuge. Each 800 µL vial was divided into 5 x 150 µL aliquots and placed into a sterile tube of the same container/closure as the original reference material. Each fraction was then frozen at −80 °C and stored until analysis using SEC, CE-SDS, and CZE.

System Suitability: All analyses were performed using bracketed analysis of an IQ standard as well as a system suitability control. The IQ standards were method dependent and are listed in the respective section below. The system suitability control was the PS prepared in parallel with the RM samples and analyzed in the same sequence. Both the IQ standard and PS were required to pass pre-defined method performance criteria determined during method qualification.

Evaluation of Uncertainty for Physicochemical Reference Values: SEC, CE-SDS, and CZE uncertainty analysis utilized a combined standard uncertainty (u_c) that incorporated PS method qualification experience. The statistical method combined the inter-vial homogeneity measured ($u^2_{iv,71}$) with a tolerance factor ($u^2_{T,PS}$) to provide the estimated combined standard uncertainty according to Equation 3:

$$u^2_{c,71} = u^2_{iv,71} + u^2_{T,PS} \tag{3}$$

where $u^2_{iv,71}$ is measured Type A uncertainty and $u^2_{T,PS}$ is a Type B uncertainty value measured during PS method qualification.

$u^2_{T,PS}$ was calculated from a one-way nested ANOVA assessment of the PS qualification data and represents the contribution of intermediate precision to the expected method variance. The square root of $u^2_{c,71}$ then yields u_c. The control range is expressed as an expanded uncertainty range of $\pm 3u_c$ for the given attributes measured.

Measurement of Size Heterogeneity by Size Exclusion Chromatography: SEC was performed using a 1.7 µm particle size, 200 Å pore size, 4.6 mm inner diameter x 150 mm length UHPLC column (Waters Corporation, P/N 186005225). The mobile phase was 100 mmol/L, pH 6.8 sodium phosphate supplemented with 250 mmol/L NaCl. Samples (6 µL) were injected onto a pre-conditioned column using a flow rate of 0.300 mL/min, resulting in a pressure of ≈180 bar. Isocratic elution was monitored for each injection using a total run time of 10 minutes. Peaks were detected by an ultraviolet absorbance variable wavelength detector at 280 nm. A gel filtration molecular weight standard was used as the instrument qualification standard.

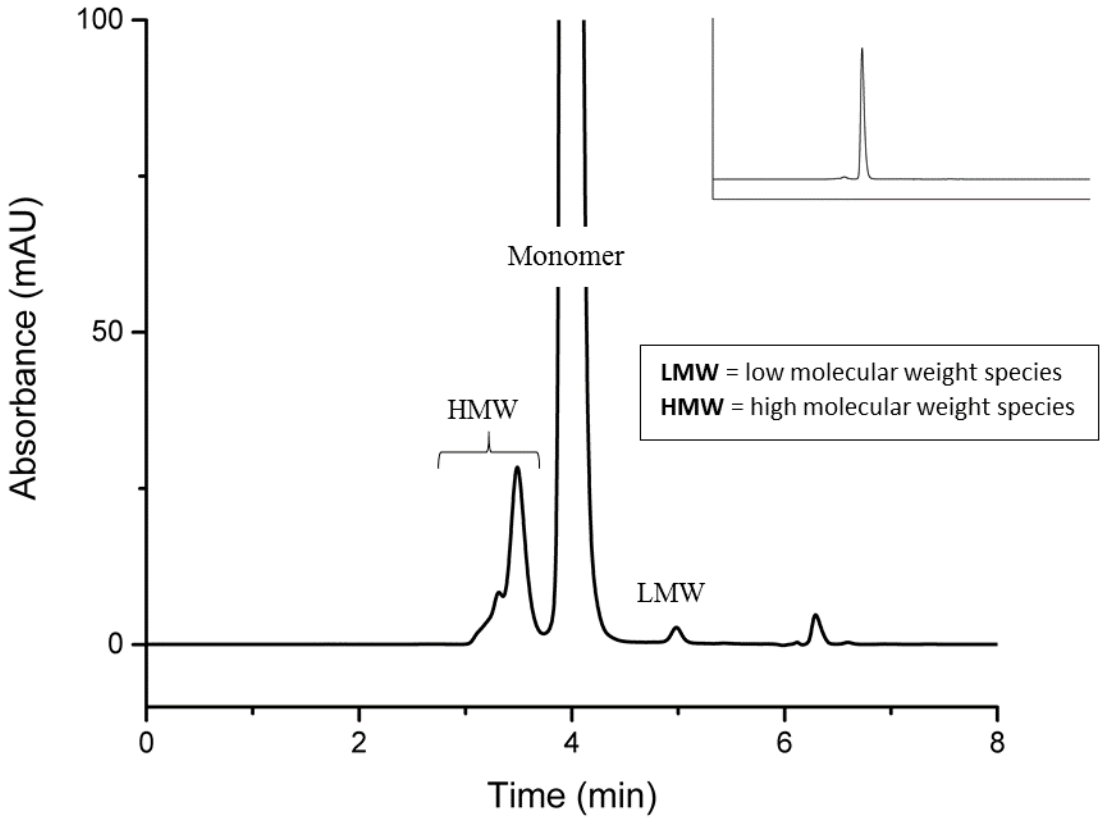

Figure 2. This chromatogram of RM 8671 Lot 14HB-D-002 is representative of the elution pattern observed with SEC. There are three main species identified as high molecular weight (HMW), monomer, and low molecular weight (LMW). Note the unlabeled peak at approximately 6.4 minutes was verified to be the void volume of the column and was due to elution of the L-histidine sample background buffer.

The parameters considered were monomeric purity (main peak relative area), HMW relative area, and LMW relative area. Preliminary analysis of the samples indicated a very slow decrease in HMW species over multiple days. It is expected that once thawed, the RM will be either refrozen or analyzed within 24 h. During the period between thawing and injection, the sample may remain in a thermostatted autosampler at a temperature between 4 °C and 10 °C. Assignment of a confidence range for this attribute therefore requires evaluation of data collected at the extremes of these expected sample handing conditions. The homogeneity values were therefore collected twice, with one sequence initiated immediately upon thawing, and a second sequence initiated after storage at 4 °C for 24 h post-thaw. Samples were stored in the autosampler during analysis at 10 °C; the samples remained in the autosampler no more than 5 h.

It should be noted that SEC results for RM 8671 do not conform to the previously observed value for PS. The relative area of the monomer has decreased from ≈98.5 % in the PS to ≈96.8 % in RM 8671 and the relative area of the high molecular weight species has increased from ≈1 % to ≈3 %, respectively. Despite a small increase in the % HMW versus PS, multiple lots of RM 8671 prepared in the same manner as Lot 14HB-D-002 have been shown to contain statistically similar main peak relative area, high molecular weight relative area and low molecular weight relative area as compared to Lot 14-HB-D-002.

Measurement of Size Heterogeneity by CE-SDS: NISTmAb monomeric purity was also measured by capillary electrophoresis sodium dodecyl sulfate (CE-SDS) under non-reducing conditions (nrCE-SDS). Glycan occupancies of the heavy chain and relative abundance of non-reducible species were measured by CE-SDS under reducing conditions (rCE-SDS). For non-reducing CE-SDS, 100 µg of NISTmAb in 10 µL of formulation buffer (10 mg/mL) were diluted to 1 mg/mL in fresh alkylating sample buffer (70 mmol/L citrate-phosphate buffer, pH 6.7, 1 % mass concentration SDS, 46 mmol/L iodoacetamide, and 1/50X 10 kDa internal standard protein). Samples were incubated for 5 min in a 70 °C water bath and cooled to room temperature prior to analysis. For reducing CE-SDS, 100 µg NISTmAb in 10 µL of formulation buffer were diluted to 1 mg/mL in fresh reducing sample buffer (70 mmol/L citrate-phosphate buffer, pH 6.7, 1 % mass concentration SDS, 5 % volume fraction 2-mercaptoethanol, 1/50X 10 kDa

internal standard protein). Samples were incubated 10 min at 70 °C in a water bath and cooled to room temperature prior to analysis. Samples were analyzed within 24 h of preparation.

All analyses were performed on a SCIEX PA800 plus capillary electrophoresis instrument fitted with a photodiode array (PDA) multi-wavelength UV detector. All separations were performed in a previously-tested bare fused silica capillary (50 µm internal diameter, 20 cm effective length, 30.5 cm total length). Samples were electrokinetically injected into the pre-conditioned capillary by applying –5 kV across the capillary for 20 s. The separation voltage (15 kV, reverse polarity) was applied for 35 min. Sample bands were detected by the fiber optic-coupled PDA detector 20 cm from the capillary inlet using absorbance at 220 nm.

Figure 3 depicts a representative non-reduced CE-SDS electropherogram collected for Lot 14HB-D-002. The dominant peak in the electropherogram can be assigned to the monomeric NISTmAb based on electrophoretic migration relative to bracketing injections of a molecular weight standard. Low abundance species corresponding to antibody fragments are also observed as indicated in Figure 3. Monomeric purity was calculated from the resultant corrected peak areas (*CA*) according to Equation 4.

$$\text{Monomeric Purity (\%)} = \frac{CA_{\text{monomer}}}{CA_{\text{monomer}} + \sum CA_{\text{fragments}}} \times 100\% \quad (4)$$

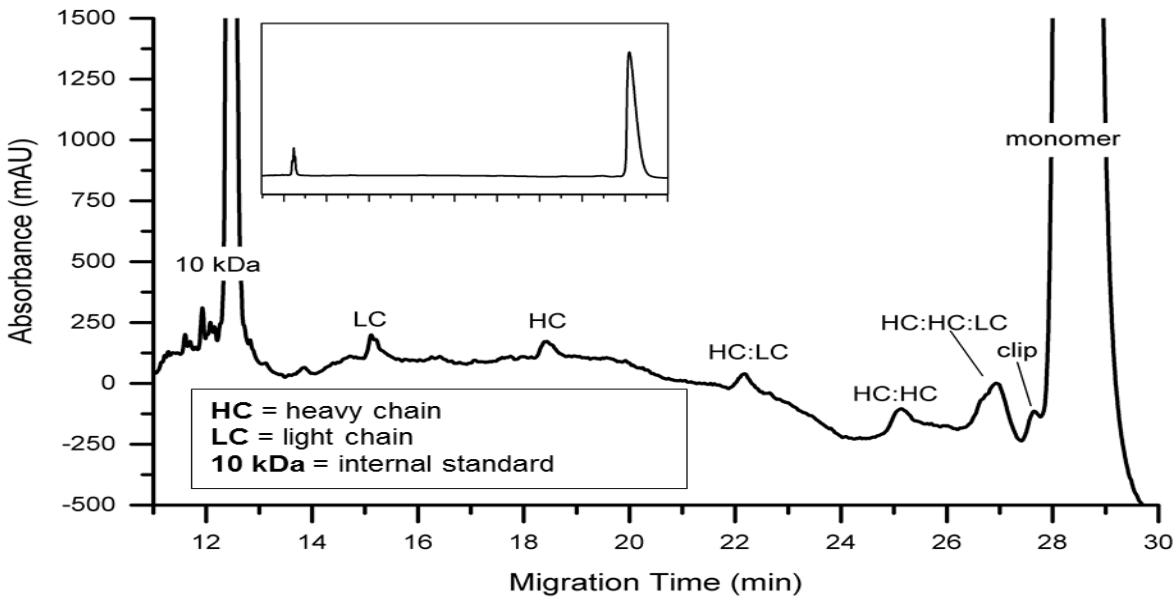

Figure 3. Representative electropherogram of RM 8671 Lot 14HB-D-002 by non-reducing CE-SDS. Clip equals the unidentified low molecular weight species peak.

Figures 4a and 4b depict a representative reduced CE-SDS electropherogram collected for Lot 14HB-D-002. The dominant peaks in the electropherogram can be assigned to the NISTmAb heavy chain and light chain based on electrophoretic migration relative to bracketing injections of a molecular weight standard. Low abundance species corresponding to aglycosylated/non-glycosylated heavy chain (NGH) and a non-reducible thioether-linked species (HC:LC thioether at heavy chain Cys223-light chain Cys213 were verified via mass spectrometry peptide mapping of a tryptic digest). For reduced samples, the relative abundance (*RA*) of each peak (LC, NGH, HC, thioether) was calculated according to Equation 5:

$$RA_X\ (\%) = \frac{CA_X}{CA_{\text{total}}} \times 100\ \% \quad (5)$$

Where (*CA*) is the corrected area for each peak "x" and CA_{total} is the sum of all corrected areas for the NISTmAb peaks.

The glycan occupancy of the heavy chain was calculated for reduced samples and system suitability controls according to Equation 6:

$$\text{Glycan Occupancy (\%)} = \frac{CA_{HC}}{CA_{HC} + CA_{NGH}} \times 100\ \% \quad (6)$$

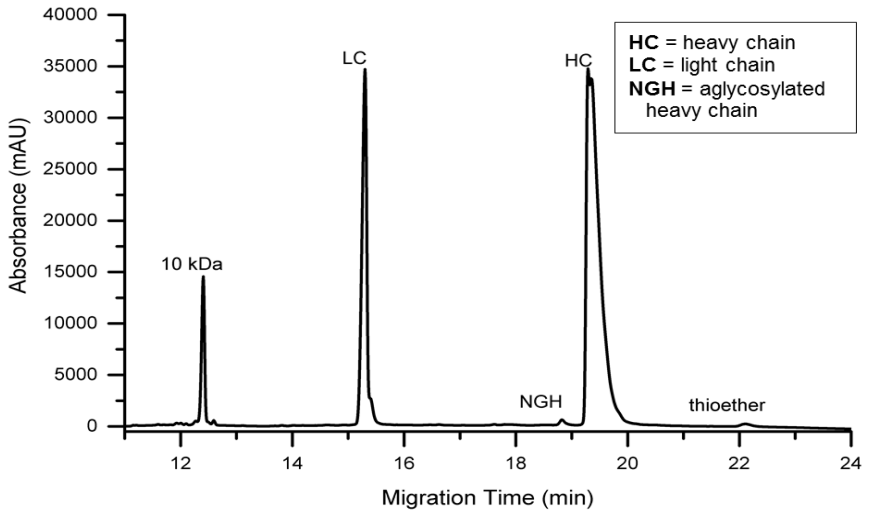

Figure 4a. This representative electropherogram of RM 8671 Lot 14HB-D-002 by reduced CE-SDS indicates the dominant peaks of the heavy and light chains based on electrophoretic migration relative to bracketing injections of a molecular weight standard. Low abundance species corresponding to a NGH and a non-reducible thioether-linked species are also identified.

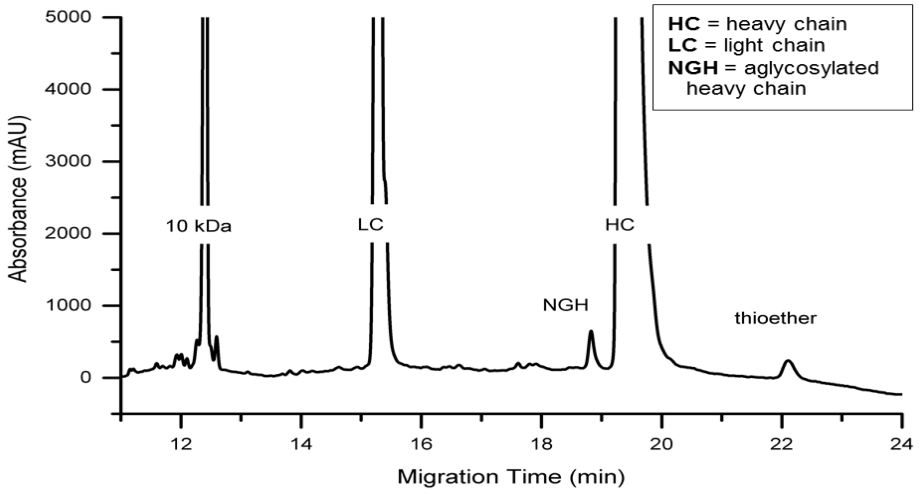

Figure 4b. Zoomed region of the electropherogram of RM 8671 Lot 14HB-D-002 by reduced CE-SDS from 13 min to 24 min.

Measurement of Charge Heterogeneity by Capillary Zone Electrophoresis: NISTmAb charge purity was measured by capillary zone electrophoresis (CZE). Samples of RM 8671 and of PS (as a system suitability control) were prepared by diluting 15 µL of sample (150 µg) with 85 µL distilled deionized (DDI) water. The instrument qualification (IQ) control was prepared by diluting 10 µL of pI 10.0 marker peptide with 90 µL DDI water.

All analyses were performed on a SCIEX PA800 plus capillary electrophoresis instrument fitted with a single-wavelength UV detector. All separations were performed in a previously-tested bare fused silica capillary (50 µm internal diameter, 40 cm effective length, 50.2 cm total length). The capillary was pre-conditioned with background electrolyte (BGE: 0.4 mol/L 6-aminocaproic acid, 2 mmol/L triethylenetetramine, 0.03 % mass concentration Tween™ 20, pH 5.7) and tested for adequate performance prior to analysis of RM 8671. Samples were hydrodynamically injected by application of 3.4 kPa pressure for 10 s (injection volume of 14 nL). The separation voltage was 30 kV (normal polarity, cathode at outlet) or +600 V/cm. Analyte bands were detected by absorbance at 214 nm by the fiber-coupled detector positioned 40 cm from the capillary inlet. All homogeneity samples were analyzed in one sequence over the course of one day.

CZE resolved the NISTmAb sample into three charge groups: the main group, which comprises the majority of the sample; the basic variants, which migrate toward the cathode more rapidly than the main group; and the acidic variants, which migrate toward the cathode less rapidly than the main charge group as shown in Figure 5. The basic variants have previously been identified as C-terminal lysine variants, with the C-terminal lysine present on either one (*) or both (**)

heavy chain subunits [17]. The acidic variants co-migrate as a smear and comprise mAb presenting a variety of post-translational modifications (PTMs), including asparagine deamidation(s), lysine glycation(s), N-terminal glutamine, and sialic acid glycovariants. The charge purity of the NISTmAb is given as the relative abundance of the main charge group with respect to all detected charge species. Charge variant relative abundance (RA) was calculated according to Equation 7 where corrected area (CA) for each peak "x" and the sum of corrected areas for all peaks (CA_{total}) were utilized:

$$RA_x(\%) = \frac{CA_x}{CA_{\text{total}}} \times 100\ \% \tag{7}$$

The charge purity is defined according to Equation 8:

$$\text{Charge Purity}\ (\%) = \frac{CA_{\text{main}}}{CA_{\text{total}}} \times 100\ \% \tag{8}$$

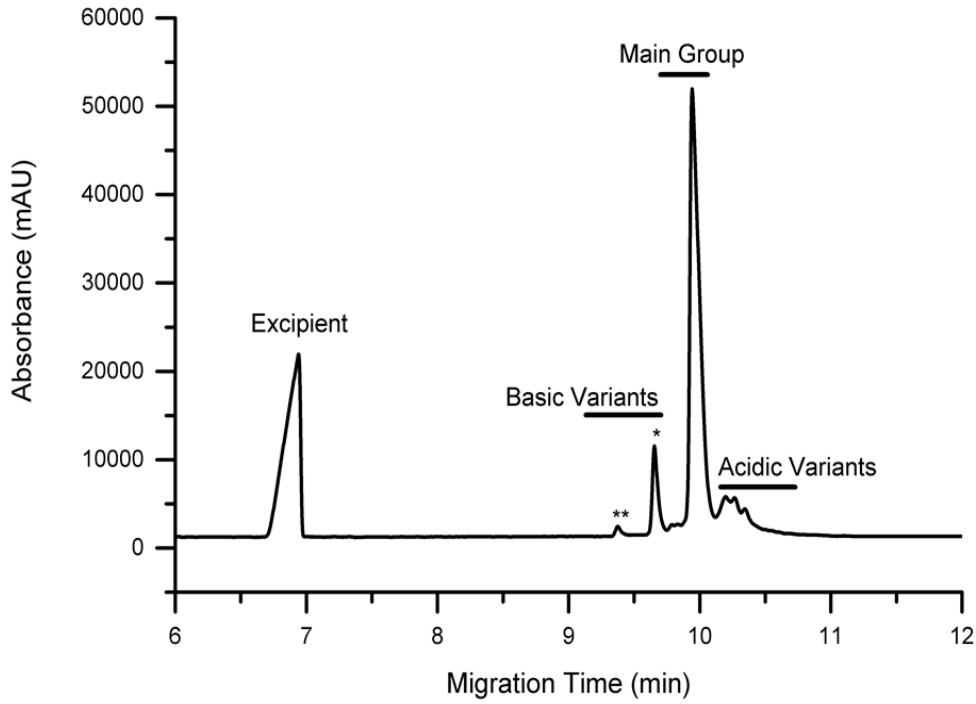

Figure 5. Representative CZE electropherogram for RM 8671 Lot 14HB-D-002 where "*" denotes the C-terminal lysine present on one HC and "**" denotes the C-terminal lysine present on both HC subunits.

Physicochemical Reference Values: The reference values listed in Tables 5, 6, and 7 are based specifically on the analytical protocols described herein. The reference values listed were determined from the average injections from three vials (n = 3 vials).

Table 5. SEC Reference Size Heterogeneity Values for RM 8671 Lot 14HB-D-002

	Size Heterogeneity (%)	Combined Standard Uncertainty, u_c (%)	Expanded Uncertainty, U (%)	Coverage Factor, k
Monomeric Purity	96.63	0.15	0.46	3
High Molecular Weight	3.17	0.15	0.45	3
Low Molecular Weight	0.20	0.008	0.024	3

Table 6. CE-SDS Reference Size Heterogeneity Values for RM 8671 Lot 14HB-D-002

	Size Heterogeneity (%)	Combined Standard Uncertainty, u_c (%)	Expanded Uncertainty, U (%)	Coverage Factor, k
Monomeric Purity[(a)]	98.47	0.79	2.38	3
Thioether[(b)]	0.30	0.02	0.06	3
Glycan Occupancy[(b)]	99.39	0.003	0.01	3

[(a)] Measured using non-reduced CE-SDS
[(b)] Measured using reduced CE-SDS

Table 7. CZE Reference Charge Heterogeneity Values for RM 8671 Lot 14HB-D-002

	Charge Heterogeneity (%)	Combined Standard Uncertainty u_c (%)	Expanded Uncertainty, U (%)	Coverage Factor, k
Charge Purity	73.82	0.17	0.52	3
Acidic Variants	16.56	0.39	1.17	3
Basic Variants	9.62	0.22	0.64	3

INFORMATIONAL VALUES AND CHARACTERIZATION DATA

Sample Handling Prior to Analysis: Each vial was thawed at room temperature and gently inverted five times.

Measurement of Hydrodynamic Diameter by Dynamic Light Scattering (DLS): DLS was used to measure the hydrodynamic diameter of RM 8671. A 200 nm diameter suspension of polystyrene beads in water was evaluated for size distribution as an IQ standard and the PS was used to demonstrate system suitability. The instrument (Malvern Zetasizer) was equipped with a backscatter detector fixed at a 173° angle, a built-in digital autocorrelator to calculate the autocorrelation function, and auto-attenuation capabilities. Each RM 8671 sample ($n = 3$ vials) was loaded (without dilution) into a clean cuvette and triplicate measurements ($n = 9$ measurements) were acquired in three successive measurements, with 10 scans, and with an equilibration time of 60 s. The viscosity of the sample was approximated to be the viscosity of water at 25 °C (0.8872 mPa·s). The refractive index of the polystyrene beads was estimated to be 1.59 and the refractive index of the protein particles was approximated to be 1.41. For each run reported, the count rates were above 2×10^5 s^{-1} with a polydispersity index (PDI) below 0.04. Zetasizer software version 7.11 was used to calculate the hydrodynamic diameter of the particles in the solution; the intensity based values were used for analysis. The information value for the Z-average observed hydrodynamic diameter of RM 8671 is provided below where triplicate measurements were performed on three different vials ($n = 9$ measurements).

Information Value for Observed Average Hydrodynamic Diameter: 9.96 nm

Measurement of Subvisible Particles Using Flow Imaging: Flow imaging was utilized to evaluate the size heterogeneity of the RM 8671 Lot 14HB-D-002 with respect to the concentration of particles with equivalent circular diameter $d \geq 2$ µm, $N(d \geq 2$ µm). Measurements were made with a ProteinSimple DPA-4200 (Set point 3, 100 µm depth flow cell). At the beginning of each day of RM 8671 analysis, 1 mL of a well-mixed solution containing nominally 5 µm beads, with a manufacturer reported concentration of 3000 mL^{-1}, were run on the instrument to assess for sizing and counting accuracy of the instrument. Additionally, PS was run prior to the test samples to obtain a baseline of protein particle counts. Prior to each analysis, the instrument's optimization protocol was performed with water.

The samples were gently inverted 5 times and each sample measured directly without further dilution or any other preparation steps. The flow cell was first primed with 0.2 mL of the sample before data acquisition to minimize dilution effects. The remaining sample flowed through at a rate of 0.1 mL/min with approximately 1760 frames being taken over the course of the run. Particle images, morphology information, size distribution, and concentrations were recorded. All PS and RM 8671 measurements, unless noted, were done in triplicate from three separate vials. These protein samples were measured directly without further dilution or any other preparation steps. The subvisible particle concentration observed for Lot 14HB-D-002 is below, for $n = 5$ vials. From the particle concentration, the amount of protein contained within the particles was estimated. From this analysis, it was determined that a negligible fraction of the monomer, compared to the concentration uncertainty from the UV-Vis experiments, is bound up in the subvisible particles.

Information Value for Subvisible Particle Concentration $N(d \geq 2$ µm): 6068 mL^{-1}

IDENTITY CONFIRMATION

Sample Handling Prior to Analysis: One vial from Lot 14HB-D-002 and one vial of PS were evaluated in parallel for primary structure confirmation. Each vial was thawed at room temperature, gently inverted five times, and spun briefly in a mini-centrifuge. Each 800 µL vial was divided into 5 x 150 µL aliquots and placed into a sterile tube of the same container/closure as the original reference material. Each fraction was then frozen at −80 °C and stored until analysis using UHPLC-UV-MS/MS peptide mapping.

Evaluation of Primary Structure Using LC-UV-MS/MS: The primary structure of the PS was exhaustively characterized in the ACS Symposium Series and the amino acid sequence shown to be consistent with that listed in Figure 6. The PS was also analyzed for the presence of low abundance sequence variants and post translational modifications [18-21].

RM 8671 Heavy Chain AA

QVTLRESGPALVKPTQTLTLTCTFSGFSLSTAGMSVGWIRQPPGKALEWLADIWWDDKKHYNPSLKDRLTIS
KDTSKNQVVLKVTNMDPADTATYYCARDMIFNFYFDVWGQGTTVTVSS ASTKGPSVFPLAPSSKSTSGGTA
ALGCLVKDYFPEPVTVSWNSGALTSGVHTFPAVLQSSGLYSLSSVVTVPSSSLGTQTYICNVNHKPSNTKVD
KRV *EPKSCDKTHTCPPCP* **APELLGGPSVFLFPPKPKDTLMISRTPEVTCVVVDVSHEDPEVKFNWYVDGV**
EVHNAKTKPREEQYNSTYRVVSVLTVLHQDWLNGKEYKCKVSNKALPAPIEKTISKAKGQPREPQVYTLPPS
REEMTKNQVSLTCLVKGFYPSDIAVEWESNGQPENNYKTTPPVLDSDGSFFLYSKLTVDKSRWQQGNVFSCS
VMHEALHNHYTQKSLSLSPGK

RM 8671 Light Chain

DIQMTQSPSTLSASVGDRVTITCSASSRVGYMHWYQQKPGKAPKLLIYDTSKLASGVPSRFSGSGSGTEFTLT
ISSLQPDDFATYYCFQGSGYPFTFGGGTKVEIK RTVAAPSVFIFPPSDEQLKSGTASVVCLLNNFYPREAKV
QWKVDNALQSGNSQESVTEQDSKDSTYSLSSTLTLSKADYEKHKVYACEVTHQGLSSPVTKSFNRGEC

Figure 6. Sequence encoded by DNA construct for RM 8671 with variable fragment antigen-binding (Fab) in normal font, constant Fab segment underlined, hinge in italics, and constant Fc in bold.

Ultrahigh-performance liquid chromatography instrumentation coupled to an ultraviolet wavelength detector and a high-resolution mass spectrometer with electrospray ionization source (UHPLC-UV-MS) were used to compare the primary structure of the PS to that of Lot 14HB-D-002 (Figure 7). The protocol utilized an optimized sample preparation workflow wherein each sample was initially diluted to approximately 1 mg/mL in denaturing buffer (6 mol/L guanidine HCl, 1 mmol/L EDTA in 0.1 mol/L Tris, pH 7.8). Dithiothreitol (5 mmol/L) was utilized for reduction of antibody disulfide bonds and iodoacetamide (IAM, 10 mmol/L) was used to alkylate the resulting free sulfhydryl groups. Samples were digested using recombinant porcine trypsin at a 1:35 enzyme:sample mass ratio for a period of 4 h at room temperature.

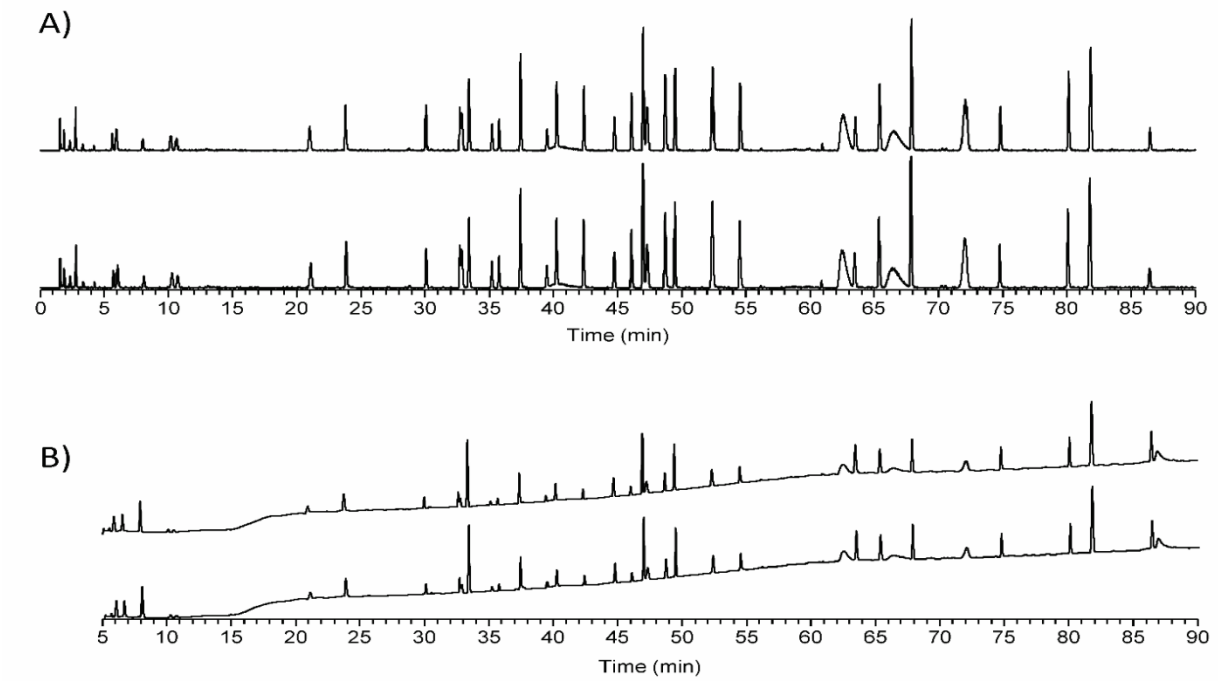

Figure 7. Representative chromatograms of the reference peptide map generated from the PS digest (top trace in panels A and B) and Lot 14HB-D-002 (bottom trace in panels A and B). The traces are representative of four injections for each sample. A comparison of the peak traces shows a high degree of similarity upon visual inspection with no trace having a unique or missing peak as compared to the PS reference map for peptide-containing peaks. The retention times for RM 8671 peaks are also highly comparable to the reference chromatogram, displaying no significant differences (< 2 %) between the means of the reference peak retention times and those of each corresponding RM 8671 peak for either TIC (A) or UV (B) chromatograms. The initial five minutes of the UV traces are not shown due to the large difference in scale between the relative levels of absorbance of peaks detected during the 0 min to 5 min period and the 5 min to 90 min period.

To further confirm the comparable identities of PS and RM 8671, MS/MS data from their tryptic digests were analyzed for peptide identification. The sequence coverage was the same for both PS and RM 8671 materials (96.89 % was achieved for the heavy chain and 100 % for the light chain) as indicated in Figure 8.

Heavy Chain (96.89 %)

```
        10         20         30         40         50         60         70         80         90
QVTLRESGPA LVKPTQTLTL TCTFSGFSLS TAGMSVGWIR QPPGKALEWL ADIWWDDKKH YNPSLKDRLT ISKDTSKNQV VLKVTNMDPA

       100        110        120        130        140        150        160        170        180
DTATYYCARD MIFNFYFDVW GQGTTVTVSS ASTKGPSVFP LAPSSKSTSG GTAALGCLVK DYFPEPVTVS WNSGALTSGV HTFPAVLQSS

       190        200        210        220        230        240        250        260        270
GLYSLSSVVT VPSSSLGTQT YICNVNHKPS NTKVDKRVEP KSCDKTHTCP PCPAPELLGG PSVFLFPPKP KDTLMISRTP EVTCVVVDVS

       280        290        300        310        320        330        340        350        360
HEDPEVKFNW YVDGVEVHNA KTKPREEQYN STYRVVSVLT VLHQDWLNGK EYKCKVSNKA LPAPIEKTIS KAKGQPREPQ VYTLPPSREE

       370        380        390        400        410        420        430        440        450
MTKNQVSLTC LVKGFYPSDI AVEWESNGQP ENNYKTTPPV LDSDGSFFLY SKLTVDKSRW QQGNVFSCSV MHEALHNHYT QKSLSLSPGK
```

Light Chain (100 %)

```
        10         20         30         40         50         60         70         80         90
DIQMTQSPST LSASVGDRVT ITCSASSRVG YMHWYQQKPG KAPKLLIYDT SKLASGVPSR FSGSGSGTEF TLTISSLQPD DFATYYCFQG

       100        110        120        130        140        150        160        170        180
SGYPFTFGGG TKVEIKRTVA APSVFIFPPS DEQLKSGTAS VVCLLNNFYP REAKVQWKVD NALQSGNSQE SVTEQDSKDS TYSLSSTLTL

       190        200        210
SKADYEKHKV YACEVTHQGL SSPVTKSFNR GEC
```

Figure 8. RM 8671 Lot 14HB-D-002 sequence coverage. RM 8671 and PS tryptic digests were analyzed by UHPLC-UV-MS/MS and sequence coverage of the heavy and light chains was calculated after peptide identification. The amino acid sequence is shown with underlining to indicate the confirmed regions.

All post translational modifications identified were consistent with those previously reported for the PS [19-20]. The mass spectrometry results indicated nearly complete pyro-glutamination of the N-terminus, moderate levels of the loss of C-terminal lysine, and low levels of glycation, oxidation, and deamidation as previously reported. No gross changes in the levels of post-translational modifications were reported compared to the PS material.

REFERENCES

[1] Schiel, J.E.; Davis, D.L.; Borisov, O.B.; *State-of-the-Art and Emerging Technologies for Therapeutic Monoclonal Antibody Characterization Volume 1. Monoclonal Antibody Therapeutics: Structure, Function, and Regulatory Space*; American Chemical Society, Vol. 1176, p. 165 (2014).

[2] Schiel, J.E.; Davis, D.L.; Borisov, O.B.; *State-of-the-Art and Emerging Technologies for Therapeutic Monoclonal Antibody Characterization Volume 3. Defining the Next Generation of Analytical and Biophysical Techniques*; American Chemical Society, Vol. 1202, p 455 (2015).

[3] Schiel, J.E.; Davis, D.L.; Borisov, O.B.; *State-of-the-Art and Emerging Technologies for Therapeutic Monoclonal Antibody Characterization Volume 2. Biopharmaceutical Characterization: The Nistmab Case Study*; American Chemical Society, Vol. 1201, p. 427 (2015).

[4] Mouchahoir, T.; Schiel, J.E.; Anal. Bioanal. Chem., Vol. 410, pp. 2111-2126 (2018).

[5] Schiel, J.E.; Turner, A.; Anal. Bioanal. Chem., Vol. 410, pp. 2067-2078 (2018).

[6] Schiel, J.E.; Turner, A.; Mouchahoir, T.; Yandrofski, K.; Telikepalli, S.; King, J.; DeRose, P.; Ripple, D.; Phinney, K.; Anal. Bioanal. Chem., Vol. 410, pp. 2127-2139 (2018).

[7] Turner, A.; Schiel, J.E.; Anal. Bioanal. Chem., Vol. 410, pp. 2079-2093 (2018).

[8] Turner, A.; Yandrofski, K.; Telikepalli, S.; King, J.; Heckert, A.; Filliben, J.; Ripple, D.; Schiel, J.E.; Anal. Bioanal. Chem., Vol. 410, pp. 2095-2110 (2018).

[9] May, W.; Parris, R.; Beck, C.; Fassett, J.; Greenberg, R.; Guenther, F.; Kramer, G.; Wise, S.; Gills, T.; Colbert, J.; Gettings, R.; Macdonald, B.; *Definitions of Terms and Modes Used at NIST for Value-Assignment of Reference Materials*; NIST Special Publication 260-136, Government Printing Office: Washington, DC (2000) available at https://www.nist.gov/system/files/documents/srm/SP260-136.PDF (accessed Dec 2020).

[10] *Iupac Compendium of Chemical Terminology*; 2nd ed.; (1997).

[11] Gokarn, Y.; Agarwal, S.; Arthur, K.; Bepperling, A.; Day, E.S.; Filoti, D.; Greene, D.G.; Hayes, D.; Kroe-Barrett, R.; Laue, T.; Lin, J.; McGarry, B.; Razinkov, V.; Singh, S.; Taing, R.; Venkataramani, S.; Weiss, W.; Yang, D.; Zarraga, I.E.; Biophysical Techniques for Characterizing the Higher Order Structure and Interactions of Monoclonal Antibodies; *State-of-the-Art and Emerging Technologies for Therapeutic Monoclonal Antibody Characterization Volume 2. Biopharmaceutical Characterization: The Nistmab Case Study*; American Chemical Society, Vol. 1201, pp 285-327 (2015).

[12] Pace, C.N.; Vajdos, F.; Fee, L.; Grimsley, G.; Gray, T. Protein Sci., Vol. 4, pp. 2411-2423 (1995).

[13] 200:2008, *J. Evaluation of Measurement Data — Guide to the Expression of Uncertainty in Measurement* (Gum 1995 with Minor Additions); Joint Committee for Guides in Metrology available at . http://www.bipm.org/utils/common/documents/jcgm/JCGM_100_2008_E.pdf (accessed Dec 2020).

[14] Travis, J.C.; Smith, M.V.; Choquette, S.J.; Liu, H.-K.; *Certified Transmittance Density Uncertainties for Standard Reference Materials Using a Transfer Spectrophotometer;* NIST Technical Reference 1715 (2015) available at https://www.nist.gov/publications/certified-transmittance-density-uncertainties-standard-reference-materials-using (accessed Dec 2020).

[15] Magnusson, B.; Ellison, S.L.; Anal. Bioanal. Chem., Vol. 390, pp. 201-213 (2008).

[16] Synek, V; *Talanta*, Vol. 65, pp. 829-837 (2005).

[17] Michels, D.A.; Ip, A.Y.; Dillon, T.M.; Brorson, K.; Lute, S.; Chavez, B.; Prentice, K.M.; Brady, L.J.; Miller, K.J.; Separation Methods and Orthogonal Techniques; *State-of-the-Art and Emerging Technologies for Therapeutic Monoclonal Antibody Characterization Volume 2. Biopharmaceutical Characterization: The Nistmab Case Study*, Schiel, J.E.; Davis, D.L.; Borisov, O.B.; Eds.; American Chemical Society, Vol. 1201, pp 237-284 (2015).

[18] Borisov, O.V.; Alvarez, M.; Carroll, J.A.; Brown, P.W.; Sequence Variants and Sequence Variant Analysis in Biotherapeutic Proteins; *State-of-the-Art and Emerging Technologies for Therapeutic Monoclonal Antibody Characterization Volume 2. Biopharmaceutical Characterization: The Nistmab Case Study*; American Chemical Society, Vol. 1201, pp 63-117 (2015).

[19] Formolo, T.; Ly, M.; Levy, M.; Kilpatrick, L.; Lute, S.; Phinney, K.; Marzilli, L.; Brorson, K.; Boyne, M.; Davis, D.; Schiel, J.; Determination of the Nistmab Primary Structure; *State-of-the-Art and Emerging Technologies for Therapeutic Monoclonal Antibody Characterization Volume 2. Biopharmaceutical Characterization: The Nistmab Case Study*; American Chemical Society, Vol. 1201, pp 1-62 (2015).

[20] Li, W.; Kerwin, J.L.; Schiel, J.; Formolo, T.; Davis, D.; Mahan, A.; Benchaar, S.A.; Structural Elucidation of Post-Translational Modifications in Monoclonal Antibodies; *State-of-the-Art and Emerging Technologies for Therapeutic Monoclonal Antibody Characterization Volume 2. Biopharmaceutical Characterization: The Nistmab Case Study*; American Chemical Society, Vol. 1201, pp 119-183 (2015).

[21] Prien, J.M.; Stöckmann, H.; Albrecht, S.; Martin, S.M.; Varatta, M.; Furtado, M.; Hosselet, S.; Wang, M.; Formolo, T.; Rudd, P.M.; Schiel, J.E.; Orthogonal Technologies for Nistmab N-Glycan Structure Elucidation and Quantitation; *State-of-the-Art and Emerging Technologies for Therapeutic Monoclonal Antibody Characterization Volume 2. Biopharmaceutical Characterization: The Nistmab Case Study;* American Chemical Society, Vol. 1201, pp. 185-235 (2015).

Report Revision History: 18 December 2020 (Change of expiration date, editorial changes); **06 October 2016** (Original report date).

Users of this RM should ensure that the Report of Investigation in their possession is current. This can be accomplished by contacting the SRM Program: telephone (301) 975-2200; e-mail srminfo@nist.gov; or via the Internet at https://www.nist.gov/srm.